Maximizing the Number of Served Users in a Smart City using Reconfigurable Intelligent Surfaces

Progress Zivuku, Steven Kisseleff, Van-Dinh Nguyen, Konstantinos Ntontin,
Wallace A. Martins, Symeon Chatzinotas, and Björn Ottersten
Interdisciplinary Centre for Security, Reliability and Trust (SnT), University of Luxembourg
E-mails: {progress.zivuku, steven.kisseleff, dinh.nguyen, kostantinos.ntontin,
wallace.alvesmartins, symeon.chatzinotas, bjorn.ottersten}@uni.lu

***Abstract*—Among a plethora of new wireless communication technologies, reconfigurable intelligent surface (RIS) emerges as one of the revolutionary solutions to provide energy- and cost-efficient signal transmissions. RIS is capable of reflecting electromagnetic signals in a controlled manner. In this paper, we jointly design the active beamforming at the base station and passive beamforming at the RIS to maximize the number of served users in a practical Smart City street scenario, subject to quality of service (QoS) and power constraints. The formulated problem belongs to the difficult class of mixed-integer non-convex programming, which is NP-hard. To arrive at a low-complexity solution, we first decompose the original problem into two sub-problems and then propose an alternating optimization algorithm based on successive convex approximation (SCA) to solve them in an iterative manner. Simulation results are provided to verify the performance improvement of the proposed algorithm as compared to baseline schemes.**

***Index Terms*—Active and passive beamforming, reconfigurable intelligent surface, smart city, successive convex approximation.**

I. Introduction

In order to meet the demand for a fully connected, intelligent and ubiquitous digital world, radically new communication technologies, network architectures, and deployment models are required. Recently, reconfigurable intelligent surface (RIS) has emerged as a promising technology for supporting massive connectivity as well as providing a cost-effective solution to achieve high spectral and energy efficiencies for wireless communication systems [1]. RIS employs controllable signal reflections, which is advantageous in complex propagation environments such as urban and city areas [2]. Signal quality with low energy consumption can be improved as RISs can intelligently reflect signals to users without amplification. As stated in [3], RISs are compatible with existing wireless network standards and hardware. Recent investigations on RISs mainly focused on application scenarios and performance metrics under different assumptions [4]. Several works investigated joint active and passive beamforming for RIS-aided networks and formulated optimization objectives, including sum rate maximization (SRM) [5], signal-to-interference-plus-noise ratio (SINR) maximization [6] and sum transmit power minimization [7].

The use of communication technologies that can promote sustainable developments is very important for future wireless networks to address the growing challenge of urbanization [8]. The integration of RISs into the Smart City concept has gained attention recently and it is quite promising for various use cases. In particular, it has potential to provide a more controllable and adaptable ecosystem for future Smart Cities. Smart City applications may involve crucial and sensitive information exchange under quality of service (QoS) constraints and minimal power consumption. A recent study in [9] discussed potential research challenges and future opportunities for the applications of RISs in Smart Cities. The advancement of connectivity and functionality in the ecosystem can be achieved by deploying RISs for coverage extension and mitigation of coverage holes, especially in the case of signal blockage. The deployment of a large number of base stations or relays to provide a sufficient coverage and QoS is typically expensive and it plays a major role in the increase of the carbon footprint of wireless communications and the radio waves emitted [10].

In this paper, we consider a scenario of a Smart City street where a crowd of users moves on a straight line toward the base station (BS). One of the key challenges of this scenario is to serve as many users as possible on the resource-constrained network. Specifically, the propagation environment does not offer sufficient angular spread to precode the interfering data streams, such that the number of users that can be served in this case is very low. In an extreme case of pure line-of-sight (LOS) propagation, the users would completely block the signals of each other, such that only the closest user can be served by the BS. To adress this problem, a RIS is deployed at a building facade of the same street. Since the position of RIS relative to the street is different than that of the base station, we can expect substantial improvements in spatial diversity using RIS, which can potentially lead to a higher number of users to be served.

The main contributions of this paper can be summarized as follows:

- We proposed a RIS-aided multi-user system which represents a challenging Smart City street scenario. This provides a more realistic scenario in the concept of Smart Cities than a circular area deployment.
- We formulate a novel optimization problem to maximize the number of served users in the network via a joint active and passive beamforming design. A user is consid-

This work is funded by the Luxembourg National Research Fund (FNR) as part of the CORE programme under project RISOTTI C20/IS/14773976.

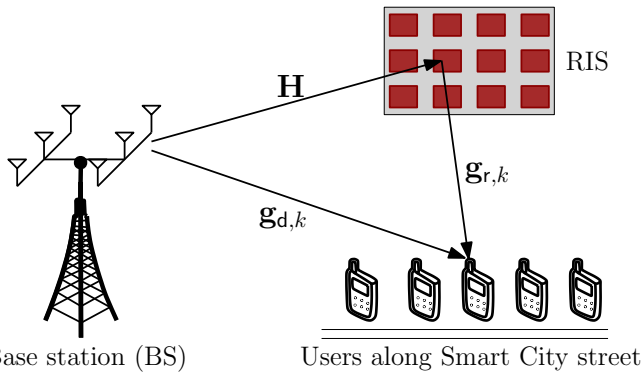

Fig. 1: RIS-aided multi-user MISO system in Smart City scenario.

ered to be successfully served if its SINR is equal to or larger than a predetermined threshold. This relationship is established by introducing binary variables in both the objective and constraints. This design strategy is more beneficial for the target application than the conventional multi-user designs based on QoS maximization or radio resource usage minimization.

- The formulated problem is a mixed-integer non-convex program, which is NP-hard. Here, we propose an alternating optimization to address this problem efficiently by decomposing it into two sub-problems and applying successive convex approximation (SCA) [11].
- Numerical results are presented to demonstrate the effectiveness of the proposed algorithm under various conditions.

The rest of the paper is organized as follows. Section II introduces the system model and optimization problem formulation. In Section III, we propose an alternating optimization algorithm to solve the formulated problem. Section IV presents the numerical results to evaluate the performance of the proposed design. Finally, we conclude the paper in Section V.

II. System Model and Optimization Problem Formulation

A. System Model

We consider a RIS-aided multi-user multiple-input single-output (MISO) system in a Smart City scenario, as illustrated in Fig. 1. There is a BS equipped with M antennas and a set $\mathcal{K} \triangleq \{1, \cdots, K\}$, of K users each equiped with single-antenna user equipment (UE). The communication between the BS and users is assisted by a RIS equipped with a set $\mathcal{N} \triangleq \{1, \cdots, N\}$ of N reflective elements deployed on a building facade. The channels from BS to RIS, BS to UE k, and RIS to UE k are denoted by $\mathbf{H} \in \mathbb{C}^{N \times M}$, $\mathbf{g}_{\mathsf{d},k} \in \mathbb{C}^{1 \times M}$, and $\mathbf{g}_{\mathsf{r},k} \in \mathbb{C}^{1 \times N}$, respectively. We consider a linear transmit beamforming at BS, where UE k is assigned a dedicated beamforming vector $\mathbf{w}_k \in \mathbb{C}^{M \times 1}$. The complex baseband signal at BS can be expressed as $\mathbf{x} = \sum_{k \in \mathcal{K}} \mathbf{w}_k s_k$, where s_k denotes the data symbol intended to UE k, which is assumed to have zero mean and unit power; in addition, s_k is assumed independent and identically distributed (i.i.d.) across k. Accordingly, the total transmit power consumed at BS is given by $P_{\text{tot}}^{\text{BS}} = \sum_{k \in \mathcal{K}} \|\mathbf{w}_k\|_2^2$. Note that $||\mathbf{w}_k||_2^2 = 0$ for all users that are not served [12]. Let $\theta_n \in [0, 2\pi]$ represent the phase shift introduced by the n-th reflective component of RIS. We denote by $\mathbf{\Theta} = \text{diag}([e^{j\theta_1} \cdots e^{j\theta_n} \cdots e^{j\theta_N}])$ the diagonal matrix which captures the reflective properties of the N reflective elements.

The received signal at UE $k \in \mathcal{K}$ can be expressed as

$$y_k = (\mathbf{g}_{\mathsf{r},k} \mathbf{\Theta} \mathbf{H} + \mathbf{g}_{\mathsf{d},k}) \sum_{i \in \mathcal{K}} \mathbf{w}_i s_i + n_k \tag{1}$$

where n_k is the additive white Gaussian noise (AWGN) at UE k with zero mean and variance σ_k^2, i.e. $n_k \sim \mathcal{CN}(0, \sigma_k^2)$. As a result, the SINR of UE $k \in \mathcal{K}$, denoted by $\gamma_k(\mathbf{w}, \boldsymbol{\theta})$, can be computed as

$$\gamma_k(\mathbf{w}, \boldsymbol{\theta}) = \frac{|(\mathbf{g}_{\mathsf{r},k} \mathbf{\Theta} \mathbf{H} + \mathbf{g}_{\mathsf{d},k}) \mathbf{w}_k|^2}{\sum\limits_{i \in \mathcal{K} \setminus \{k\}} |(\mathbf{g}_{\mathsf{r},k} \mathbf{\Theta} \mathbf{H} + \mathbf{g}_{\mathsf{d},k}) \mathbf{w}_i|^2 + \sigma_k^2} \tag{2}$$

where $\mathbf{w} \triangleq [\mathbf{w}_k]_{k \in \mathcal{K}}$ and $\boldsymbol{\theta} \triangleq [\theta_n]_{n \in \mathcal{N}}$.

B. Optimization Problem Formulation

The main goal of this work is to maximize the number of users to be served, subject to a predetermined SINR threshold, denoted by γ_{th}. We introduce binary variables $\boldsymbol{\epsilon} \triangleq \{\epsilon_k\}_{k \in \mathcal{K}}$ to establish the state of each user as follows:

$$\epsilon_k = \begin{cases} 1, & \text{if UE } k \text{ is successfully served;} \\ 0, & \text{otherwise.} \end{cases} \tag{3}$$

Definition 1. *The value of ϵ_k is equal to one if the condition $\gamma_k(\mathbf{w}, \boldsymbol{\theta}) \geq \gamma_{\text{th}}$ is satisfied; otherwise $\epsilon_k = 0$. This relationship is generally expressed as $\gamma_k(\mathbf{w}, \boldsymbol{\theta}) \geq \epsilon_k \gamma_{\text{th}}$ with $\epsilon_k \in \{0, 1\}$.*

Based on the above discussions and definition, the joint active and passive beamforming optimization problem for maximizing the number of served users can be mathematically formulated as

$$\mathscr{P}: \quad \max_{\mathbf{w}, \boldsymbol{\theta}, \boldsymbol{\epsilon}} \sum_{k \in \mathcal{K}} \epsilon_k \tag{4a}$$

$$\text{s. t.} \quad \gamma_k(\mathbf{w}, \boldsymbol{\theta}) \geq \epsilon_k \gamma_{\text{th}}, \ \forall k \in \mathcal{K} \tag{4b}$$

$$\sum_{k \in \mathcal{K}} \|\mathbf{w}_k\|_2^2 \leq P^{\max} \tag{4c}$$

$$0 \leq \theta_n \leq 2\pi, \ \forall n \in \mathcal{N} \tag{4d}$$

$$\epsilon_k \in \{0, 1\}, \ \forall k \in \mathcal{K} \tag{4e}$$

where $P^{\max}$ is the power budget at the BS.

III. Proposed Alternating Optimization Algorithm

Challenges of solving problem $\mathscr{P}$: The problem described in (4) is a mixed-integer non-convex programming due to the non-convexity of constraint (4b) and the binary nature of constraint (4e), thus making rather challenging to solve $\mathscr{P}$ directly. To address these challenges, we first relax binary variables to continuous ones (i.e. $\epsilon_k \in [0, 1], \forall k$), and slightly reformulate problem (4), which allows us to split it into two sub-problems and apply SCA to each of them.

A. Tractable Problem Formulation

The relaxed formulation for the problem in (4) is

$$\max_{\mathbf{w},\boldsymbol{\theta},\boldsymbol{\epsilon}} \sum_{k\in\mathcal{K}} \epsilon_k \tag{5a}$$

$$\text{s. t.} \quad 0 \le \epsilon_k \le 1,\ \forall k \in \mathcal{K} \tag{5b}$$

$$(4b), (4c), (4d). \tag{5c}$$

We note that any feasible point of problem (5) is also feasible to problem (4), but not vice versa. The equivalence between (4) and (5) is guaranteed by considering additional constraints: $\epsilon_k - \epsilon_k^2 \le 0,\ \forall k$, which is equivalent to $\epsilon_k \in (-\infty, 0] \cup [1, +\infty), \forall k$. Therefore, the inequalities $\epsilon_k - \epsilon_k^2 \le 0$ and (5b) hold true simultaneously only if ϵ_k is binary. As a result, problem (4) is equivalent to

$$\max_{\mathbf{w},\boldsymbol{\theta},\boldsymbol{\epsilon}} \sum_{k\in\mathcal{K}} \epsilon_k \tag{6a}$$

$$\text{s. t.} \quad 0 \le \epsilon_k \le 1,\ \forall k \in \mathcal{K} \tag{6b}$$

$$\epsilon_k - \epsilon_k^2 \le 0,\ \forall k \in \mathcal{K} \tag{6c}$$

$$(4b), (4c), (4d). \tag{6d}$$

It is noted that constraint (6c) will make problem (6) infeasible in most cases for $\epsilon_k \in [0, 1]$.

Parameterized relaxed problem: Inspired by [13], we introduce the following penalty function:

$$\mathcal{P}(\boldsymbol{\epsilon}, \mu) = \mu\big(\sum_{k\in\mathcal{K}} \epsilon_k^2 - \sum_{k\in\mathcal{K}} \epsilon_k\big) \triangleq \mu\big(h(\boldsymbol{\epsilon}) - g(\boldsymbol{\epsilon})\big) \tag{7}$$

which can be used to bypass constraint (6c) and improve the convergence rate of the proposed iterative algorithm. The positive constant μ in (7) is a penalty parameter that is used to obtain near-optimal binary points at convergence.

Lemma 1. *With an appropriate value of the penalty parameter μ, problem* (6) *(or the original problem* (4)*) is equivalent to the following parameterized relaxed problem:*

$$\min_{\mathbf{w},\boldsymbol{\theta},\boldsymbol{\epsilon}} \quad \psi(\boldsymbol{\epsilon}) = -\sum_{k\in\mathcal{K}} \epsilon_k - \mu\big(h(\boldsymbol{\epsilon}) - g(\boldsymbol{\epsilon})\big) \tag{8a}$$

$$\text{s. t.} \quad 0 \le \epsilon_k \le 1,\ \forall k \in \mathcal{K} \tag{8b}$$

$$(4b), (4c), (4d). \tag{8c}$$

The proof follows the same procedure as outlined in [13]. It is apparent that $h(\boldsymbol{\epsilon}) - g(\boldsymbol{\epsilon}) = 0$ must hold at optimum with a proper value of μ; otherwise, we can increase μ until the penalty value is close to zero. This implies that there always exists a positive penalty parameter μ to obtain a solution.

In the following, we focus on solving the parameterized relaxed problem (8) instead of the original problem (4). However, a direct application of SCA method is still inapplicable due to the complicated SINR rate function. More importantly, there may exist some $\epsilon_k = 0$, but their corresponding SINR is still larger than zero. In other words, there exists small values of $\|\mathbf{w}_k\|_2^2$ for some $\epsilon_k = 0$, but not negligible, making resource utilization less efficient. To overcome these issues, we introduce new variables $\boldsymbol{\omega} \triangleq \{\omega_k\}_{k\in\mathcal{K}}$ and $\boldsymbol{\varphi} \triangleq \{\varphi_k\}_{k\in\mathcal{K}}$ to equivalently rewrite problem (8) as

$$\min_{\mathbf{w},\boldsymbol{\theta},\boldsymbol{\epsilon},\boldsymbol{\omega},\boldsymbol{\varphi}} \ \psi(\boldsymbol{\epsilon}) = -\sum_{k\in\mathcal{K}} \epsilon_k - \mu\big(h(\boldsymbol{\epsilon}) - g(\boldsymbol{\epsilon})\big) \tag{9a}$$

$$\text{s. t.} \quad \gamma_{\text{th}}\epsilon_k - \frac{|\mathbf{h}_k\mathbf{w}_k|^2}{\varphi_k} \le 0,\ \forall k \in \mathcal{K} \tag{9b}$$

$$\sum_{i\in\mathcal{K}\setminus\{k\}} |\mathbf{h}_k\mathbf{w}_i|^2 + 1 \le \varphi_k,\ \forall k \in \mathcal{K} \tag{9c}$$

$$\sum_{i\in\mathcal{K}} \omega_k \le P^{\max},\ \forall k \in \mathcal{K} \tag{9d}$$

$$\|\mathbf{w}_k\|_2^2 \le \epsilon_k\omega_k,\ \forall k \in \mathcal{K} \tag{9e}$$

$$(4d), (8b) \tag{9f}$$

where $\mathbf{h}_k$ denotes the normalized effective channel between BS and UE k, which is defined as $\mathbf{h}_k \triangleq (\mathbf{g}_{\mathsf{r},k}\boldsymbol{\Theta}\mathbf{H} + \mathbf{g}_{\mathsf{d},k})/\sigma$. Here, φ_k and ω_k are used to bound the sum interference power and beamforming power at UE k, respectively. It can be seen that whenever $\epsilon_k = 0$, we have $\|\mathbf{w}_k\|_2^2 = 0$ due to constraint (9e). In problem (9), the non-convex parts include the objective (9a) and constraint (9b). We note that constraint (9e) can be cast into a second-order cone constraint as:

$$(9e) \Leftrightarrow \|[\mathbf{w}_k,\ 0.5(\epsilon_k - \omega_k)]\|_2 \le 0.5(\epsilon_k + \omega_k),\ \forall k \in \mathcal{K}. \tag{10}$$

B. Proposed Alternating Descent-based SCA Algorithm

For an SCA-based iterative algorithm similar to [11], let us denote by $(\mathbf{w}^{(\tau)}, \boldsymbol{\theta}^{(\tau)}, \boldsymbol{\epsilon}^{(\tau)}, \boldsymbol{\varphi}^{(\tau)})$ the feasible point of (9) obtained at iteration $\tau - 1$. We are now in position to apply SCA method to iteratively solve (9) in an alternating manner. In particular, at iteration $\tau+1$, we solve problem (9) for given $\boldsymbol{\theta}^{(\tau)}$ to find the optimal solution $(\mathbf{w}^*, \boldsymbol{\epsilon}^*, \boldsymbol{\varphi}^*, \boldsymbol{\omega}^*)$, and then solve (9) for given $\mathbf{w}^{(\tau+1)} := \mathbf{w}^*$.

Active Beamforming Descent Iteration: At iteration $\tau + 1$, we rewrite problem (9) for given $\boldsymbol{\theta}^{(\tau)}$ as

$$\mathscr{P}_{\mathbf{w}}: \min_{\mathbf{w},\boldsymbol{\epsilon},\boldsymbol{\omega},\boldsymbol{\varphi}} \ \psi_{\mathbf{w}}(\boldsymbol{\epsilon}) \triangleq -\sum_{k\in\mathcal{K}} \epsilon_k - \mu\big(h(\boldsymbol{\epsilon}) - g(\boldsymbol{\epsilon})\big) \tag{11a}$$

$$\text{s. t.} \quad \gamma_{\text{th}}\epsilon_k - \frac{|\mathbf{h}_k\mathbf{w}_k|^2}{\varphi_k} \le 0,\ \forall k \in \mathcal{K} \tag{11b}$$

$$(8b), (9c), (9d), (10). \tag{11c}$$

To tackle the non-convexity of (11a), we need to approximate the convex function $h(\boldsymbol{\epsilon}) \triangleq \sum_{k\in\mathcal{K}} \epsilon_k^2$ which is quadratic. We apply the first-order Taylor approximation to obtain a lower bound approximation around the feasible point $\boldsymbol{\epsilon}^{(\tau)}$ as

$$\begin{aligned} h(\boldsymbol{\epsilon}) &\ge h(\boldsymbol{\epsilon}^{(\tau)}) + \nabla_{\boldsymbol{\epsilon}^{(\tau)}} h(\boldsymbol{\epsilon})^T(\boldsymbol{\epsilon} - \boldsymbol{\epsilon}^{(\tau)}) \\ &= \sum_{k\in\mathcal{K}} \Big(2\epsilon_k^{(\tau)}\epsilon_k - (\epsilon_k^{(\tau)})^2\Big) := h^{(\tau)}(\boldsymbol{\epsilon}; \boldsymbol{\epsilon}^{(\tau)}) \end{aligned} \tag{12}$$

where $h^{(\tau)}(\boldsymbol{\epsilon}; \boldsymbol{\epsilon}^{(\tau)})$ is a linear function in $\boldsymbol{\epsilon}$, satisfying $h(\boldsymbol{\epsilon}) \ge h^{(\tau)}(\boldsymbol{\epsilon}; \boldsymbol{\epsilon}^{(\tau)})$ and $h(\boldsymbol{\epsilon}^{(\tau)}) = h^{(\tau)}(\boldsymbol{\epsilon}^{(\tau)}; \boldsymbol{\epsilon}^{(\tau)})$ whenever $\boldsymbol{\epsilon}^{(\tau)} = \boldsymbol{\epsilon}^{(\tau-1)}$. As a result, the objective (11a) is iteratively replaced by the following linear function

$$\psi_{\mathbf{w}}^{(\tau)}(\boldsymbol{\epsilon}) \triangleq -\sum_{k\in\mathcal{K}} \epsilon_k - \mu\big(h^{(\tau)}(\boldsymbol{\epsilon}; \boldsymbol{\epsilon}^{(\tau)}) - g(\boldsymbol{\epsilon})\big). \tag{13}$$

Next, we can see that the quadratic-over-linear function $\gamma_k(\mathbf{w}_k, \varphi_k) \triangleq |\mathbf{h}_k\mathbf{w}_k|^2/\varphi_k$ in constraint (11b) is convex, which is useful to approximate by SCA method. The global lower bound of $\gamma_k(\mathbf{w}_k, \varphi_k)$ around the feasible point $(\mathbf{w}_k^{(\tau)}, \varphi_k^{(\tau)})$ is given by [14, Eq. (21)]

$$\gamma_k(\mathbf{w}_k, \varphi_k) \ge \frac{2\Re\Big\{(\mathbf{w}_k^{(\tau)})^H\mathbf{h}_k^H\mathbf{h}_k\mathbf{w}_k\Big\}}{\varphi_k^{(\tau)}} - \frac{|\mathbf{h}_k\mathbf{w}_k^{(\tau)}|^2}{(\varphi_k^{(\tau)})^2}\varphi_k$$

$$:= \gamma_k^{(\tau)}(\mathbf{w}_k, \varphi_k; \mathbf{w}_k^{(\tau)}, \varphi_k^{(\tau)}). \quad (14)$$

Thus, the non-convex constraint (11b) is iteratively replaced by the following convex one:

$$\gamma_{\text{th}}\epsilon_k - \gamma_k^{(\tau)}(\mathbf{w}_k, \varphi_k; \mathbf{w}_k^{(\tau)}, \varphi_k^{(\tau)}) \leq 0, \ \forall k \in \mathcal{K}. \quad (15)$$

Simply put, we solve the following approximate convex program of (11) at iteration $\tau + 1$:

$$\min_{\mathbf{w},\boldsymbol{\epsilon},\boldsymbol{\omega},\boldsymbol{\varphi}} \ \psi_{\mathbf{w}}^{(\tau)}(\boldsymbol{\epsilon}) \triangleq -\sum_{k\in\mathcal{K}} \epsilon_k - \mu\big(h^{(\tau)}(\boldsymbol{\epsilon};\boldsymbol{\epsilon}^{(\tau)}) - g(\boldsymbol{\epsilon})\big) \quad (16a)$$

$$\text{s. t.} \ \ \gamma_{\text{th}}\epsilon_k - \gamma_k^{(\tau)}(\mathbf{w}_k, \varphi_k; \mathbf{w}_k^{(\tau)}, \varphi_k^{(\tau)}) \leq 0, \forall k \in \mathcal{K} \quad (16b)$$

$$(8b), (9c), (9d), (10). \quad (16c)$$

In an iterative algorithm presented shortly, the worst-case computational complexity per iteration of solving (16) by the interior-point method is $\mathcal{O}\big(\sqrt{5K}(MK+3K)^3\big)$ [15, Chapter 6].

Phase Shift Descent Iteration: At iteration $\tau+1$, we rewrite problem (9) for given $\mathbf{w}^{(\tau)}$ as

$$\mathscr{P}_{\boldsymbol{\theta}}: \min_{\boldsymbol{\theta},\boldsymbol{\epsilon},\boldsymbol{\varphi}} \ \psi_{\boldsymbol{\theta}}(\boldsymbol{\epsilon}) \triangleq -\sum_{k\in\mathcal{K}} \epsilon_k - \mu\big(h(\boldsymbol{\epsilon}) - g(\boldsymbol{\epsilon})\big) \quad (17a)$$

$$\text{s. t.} \ \gamma_{\text{th}}\epsilon_k - \gamma_k(\boldsymbol{\theta}, \varphi_k) \leq 0, \ \forall k \in \mathcal{K} \quad (17b)$$

$$(4d), (8b), (9c) \quad (17c)$$

where $\gamma_k(\boldsymbol{\theta}, \varphi_k) \triangleq \dfrac{|(\mathbf{g}_{\mathsf{r},k}\boldsymbol{\Theta}\mathbf{H} + \mathbf{g}_{\mathsf{d},k})\mathbf{w}_k|^2}{\sigma^2\varphi_k}$. The non-convex parts include (17a) and (17b). We note that the objective (17a) is already convexified in (13), while constraint (17b) can be approximated similar to (16b). In particular, constraint (17b) is iteratively replaced by the following convex one:

$$\gamma_{\text{th}}\epsilon_k - \gamma_k^{(\tau)}(\boldsymbol{\theta}, \varphi_k; \boldsymbol{\theta}^{(\tau)}, \varphi_k^{(\tau)}) \leq 0, \ \forall k \in \mathcal{K} \quad (18)$$

where $\gamma_k^{(\tau)}(\boldsymbol{\theta}, \varphi_k; \boldsymbol{\theta}^{(\tau)}, \varphi_k^{(\tau)})$ is the global lower bound of $\gamma_k(\boldsymbol{\theta}, \varphi_k)$, which is given as

$$\gamma_k^{(\tau)}(\boldsymbol{\theta}, \varphi_k; \boldsymbol{\theta}^{(\tau)}, \varphi_k^{(\tau)}) \triangleq \frac{2\Re\Big\{\mathbf{w}_k^H(\mathbf{g}_{\mathsf{r},k}\boldsymbol{\Theta}^{(\tau)}\mathbf{H} + \mathbf{g}_{\mathsf{d},k})^H(\mathbf{g}_{\mathsf{r},k}\boldsymbol{\Theta}\mathbf{H} + \mathbf{g}_{\mathsf{d},k})\mathbf{w}_k\Big\}}{\sigma^2\varphi_k} - \frac{|(\mathbf{g}_{\mathsf{r},k}\boldsymbol{\Theta}^{(\tau)}\mathbf{H} + \mathbf{g}_{\mathsf{d},k})\mathbf{w}_k|^2}{\big(\sigma\varphi_k^{(\tau)}\big)^2}\varphi_k. \quad (19)$$

The approximate convex program of (17) at iteration $\tau+1$ is given by

$$\min_{\boldsymbol{\theta},\boldsymbol{\epsilon},\boldsymbol{\varphi}} \ \psi_{\boldsymbol{\theta}}^{(\tau)}(\boldsymbol{\epsilon}) \triangleq -\sum_{k\in\mathcal{K}} \epsilon_k - \mu\big(h^{(\tau)}(\boldsymbol{\epsilon};\boldsymbol{\epsilon}^{(\tau)}) - g(\boldsymbol{\epsilon})\big) \quad (20a)$$

$$\text{s. t.} \ \gamma_{\text{th}}\epsilon_k - \gamma_k^{(\tau)}(\boldsymbol{\theta}, \varphi_k; \boldsymbol{\theta}^{(\tau)}, \varphi_k^{(\tau)}) \leq 0, \forall k \in \mathcal{K} \quad (20b)$$

$$(4d), (8b), (9c) \quad (20c)$$

which requires the computational complexity per iteration $\mathcal{O}\big(\sqrt{3K+M}(M+2K)^3\big)$. The overall iterative algorithm is described using pseudo code notation in Alg. 1.

Convergence analysis: Here we briefly provide the convergence analysis of Algorithm 1 based on SCA properties. From (16) and (20), one can show that $\psi_{\mathbf{w}}(\boldsymbol{\epsilon}^{(\tau+1)}|\mathbf{w}^{(\tau+1)}, \boldsymbol{\theta}^{(\tau)}) \leq \psi_{\mathbf{w}}^{(\tau)}(\boldsymbol{\epsilon}^{(\tau+1)}|\mathbf{w}^{(\tau+1)}, \boldsymbol{\theta}^{(\tau)}) \leq \psi_{\mathbf{w}}^{(\tau)}(\boldsymbol{\epsilon}^{(\tau)}|\mathbf{w}^{(\tau)}, \boldsymbol{\theta}^{(\tau)}) = \psi_{\mathbf{w}}(\boldsymbol{\epsilon}^{(\tau)}|\mathbf{w}^{(\tau)}, \boldsymbol{\theta}^{(\tau)})$ and $\psi_{\boldsymbol{\theta}}(\boldsymbol{\epsilon}^{(\tau+1)}|\mathbf{w}^{(\tau+1)}, \boldsymbol{\theta}^{(\tau+1)}) \leq \psi_{\boldsymbol{\theta}}^{(\tau)}(\boldsymbol{\epsilon}^{(\tau+1)}|\mathbf{w}^{(\tau+1)}, \boldsymbol{\theta}^{(\tau+1)}) \leq \psi_{\boldsymbol{\theta}}^{(\tau)}(\boldsymbol{\epsilon}^{(\tau)}|\mathbf{w}^{(\tau+1)}, \boldsymbol{\theta}^{(\tau)}) = \psi_{\boldsymbol{\theta}}(\boldsymbol{\epsilon}^{(\tau)}|\mathbf{w}^{(\tau+1)}, \boldsymbol{\theta}^{(\tau)})$.

Algorithm 1 Alternating Descent-based Algorithm

Initialization: Set $\tau = 1$ and randomly initialized feasible points for $(\mathbf{w}^{(0)}, \boldsymbol{\theta}^{(0)}, \boldsymbol{\epsilon}^{(0)}, \boldsymbol{\varphi}^{(0)})$ to constraints in (9)

1: **repeat**
2: Solve (16) for given $\boldsymbol{\theta}^{\tau}$ to obtain the optimal solutions $(\mathbf{w}^*, \boldsymbol{\epsilon}^*, \boldsymbol{\varphi}^*, \boldsymbol{\omega}^*)$ and update $(\mathbf{w}^{(\tau+1)}, \boldsymbol{\epsilon}^{(\tau+1)}, \boldsymbol{\varphi}^{(\tau+1)}) := (\mathbf{w}^*, \boldsymbol{\epsilon}^*, \boldsymbol{\varphi}^*)$;
3: Solve (20) for given $(\mathbf{w}^{(\tau+1)}, \boldsymbol{\epsilon}^{(\tau+1)}, \boldsymbol{\varphi}^{(\tau+1)}))$ to obtain the optimal solutions $(\boldsymbol{\theta}^*, \boldsymbol{\epsilon}^*, \boldsymbol{\varphi}^*)$ and update $(\boldsymbol{\theta}^{(\tau+1)}, \boldsymbol{\epsilon}^{(\tau+1)}, \boldsymbol{\varphi}^{(\tau+1)}) := (\boldsymbol{\theta}^*, \boldsymbol{\epsilon}^*, \boldsymbol{\varphi}^*)$;
4: Set $\tau = \tau + 1$;
5: **until** Convergence
6: **Output:** $(\mathbf{w}^*, \boldsymbol{\theta}^*, \boldsymbol{\epsilon}^*)$.

This implies that Algorithm 1 generates a sequence $\{\mathbf{w}^{(\tau)}, \boldsymbol{\theta}^{(\tau)}, \boldsymbol{\epsilon}^{(\tau)}, \boldsymbol{\varphi}^{(\tau)}\}$ of improved points with respect to the objective function of problem (8). Accordingly, the parameter set converges to a local optimal solution.

Choice of the penalty parameter μ: An appropriate value of μ is important to guarantee the overall system performance of Algorithm 1. We can easily observe that a large value of μ may speed up the convergence of Algorithm 1 and guarantee an exact binary solution, but this will also result in a huge performance loss due to an inappropriate convergence. Unlike [13], both the original objective and penalty function in problem (8) are a function of $\boldsymbol{\epsilon}$, which makes the penalty process more efficient even for a small value of μ. In our simulations, we have observed that $\mu = 0.2$ is the most suitable value that ensures the convergence of Algorithm 1 with an exact binary solution, while achieving the best performance.

IV. Numerical Results

The considered scenario of a Smart City street is illustrated in Fig. 2. The key simulation parameters are given in Table I, following studies in [16]–[19].

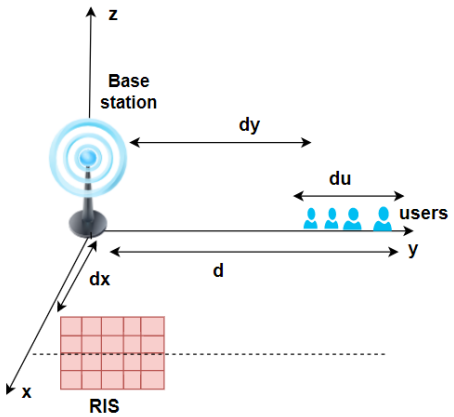

Fig. 2: The considered scenario of a Smart City street.

We assume that BS is located at the origin and users are uniformly distributed at random in the y-axis between 30 m and 50 m. The RIS is deployed dx distance on the side of the street. However, its position in y-direction can be

TABLE I: Simulation Parameters

Parameter	Value
Carrier frequency (f_c)	2.4 GHz
Noise power (σ^2)	-80 dBm
SINR threshold (γ_{th})	10 dB
Transmission power ($P^{\max}$)	20 dBm
BS height	3 m
User equipment height	1.5 m
RIS deployment height	3 m
BS-UE minimum distance	30 m
BS-UE maximum distance	50 m
RIS dx distance	5 m
BS to RIS pathloss exponent ($\alpha_{\text{bs-ris}}$)	2.3
RIS to user pathloss exponent ($\alpha_{\text{ris-user}}$)	2.7
BS to user pathloss exponent ($\alpha_{\text{bs-user}}$)	2.7
Antenna and element spacing	0.5λ

varied. An independent Rician channel fading is considered for all the channels with the Rician factor β. Note that RIS is deployed with the knowledge of the BS' location and is typically placed higher than users. Thus, less scattering from the users themselves is expected, and thus, we set $\alpha_{\text{bs-ris}} < \alpha_{\text{bs-user}}$ [18]. The stopping threshold for Algorithm 1 is set to 10^{-3} and the number of RIS reflective elements is fixed at $N = 1000$ for all simulations. In the following, all the simulation results are averaged over 10^3 channel realizations. To verify the effectiveness of the proposed algorithm, we compare the proposed solution with the following two baseline schemes:

- Without RIS: The users are served directly by BS.
- RIS with random phase: The phase shifts are not optimized, such that RIS represents a scatterer. While RIS is not capable of beamforming the signals toward users, it may still create additional signal paths to enhance the spatial diversity.

The solutions of these two baseline schemes can be easily obtained using Algorithm 1 with small simplifications.

A. The Optimal RIS Position in the Considered Scenario

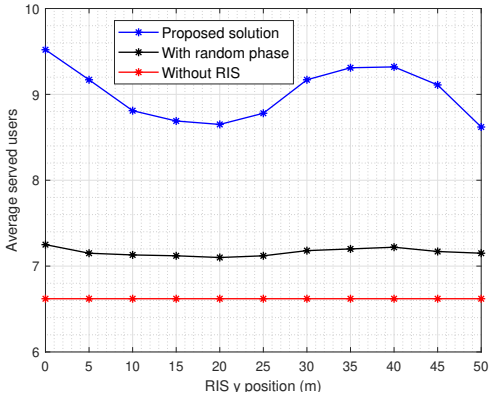

Fig. 3: Average number of served users with varying RIS position.

In this subsection, we make an analysis of the possible RIS deployment positions to obtain better performance in the proposed scenario.

At first, we assume that the Rician factor (β) is fixed and equal to 3 dB for all links and $M = K = 10$. As depicted in Fig. 3, we observe that employing RIS (Proposed solution) with optimized reflective coefficients substantially outperforms the two benchmarks. Moreover, we observe that there are two peaks for the proposed solution, i.e. at d = 0 m and d = 40 m. While this behavior is known from previous works on RIS-assisted communications, e.g. [20], the asymmetry of this curve is a new observation. It results from the distribution of the users, such that the same position of RIS can be optimal for one user and suboptimal for another. Accordingly, the peak of the curve that is close to the users' locations is wider and lower compared to the peak associated with the deployment of RIS in proximity of the BS. Another important observation is that a random scatterer can still increase the probability of serving more users. However, the performance of this benchmark scheme remains rather close to the other benchmark without RIS.

B. Analysis of Served Users with Varying Rician Factor

In this subsection, we study the effect of Rician factor on the average served users.

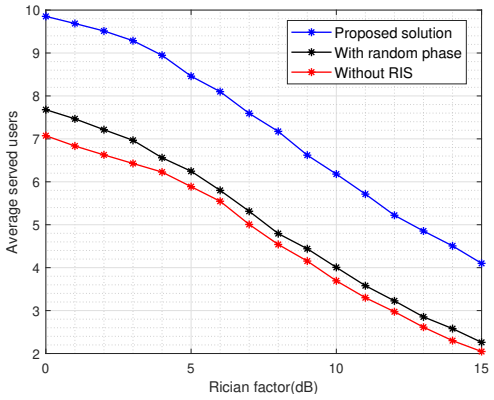

Fig. 4: Average number of served users with varying Rician.

We position the RIS at $d = 0$ m for this analysis and vary β from 0 dB to 15 dB. We set $M = K = 10$. As shown in Fig. 4, the proposed solution provides an increase in the performance as compared to the two baseline schemes. While there is a noticeable performance gap between the proposed solution and the baseline schemes, the number of average users served decreases as the Rician factor increases. For the benchmark without RIS, with increasing Rician factor less and less diversity is left in the channel matrix, such that as the users move on a street, the signals to the distant users are more and more blocked by the users in front. Accordingly, the experienced signal quality reduces. Similarly for the RIS-assisted link, the performance decreases as the diversity reduces, i.e. the channel becomes a pure line-of-sight (LoS) propagation channel. Accordingly, less diversity

is available to produce independent beams with a sufficient signal quality.

C. Analysis of Average Served Users versus Number of Users

Next, we set $M = 16$ and vary the total number of users on the street from $K = 2$ to $K = 16$. The results are depicted in Fig. 5. We position the RIS at $d = 0$ m and set $\beta = 3$ dB. It can be noted that with a low number of users the

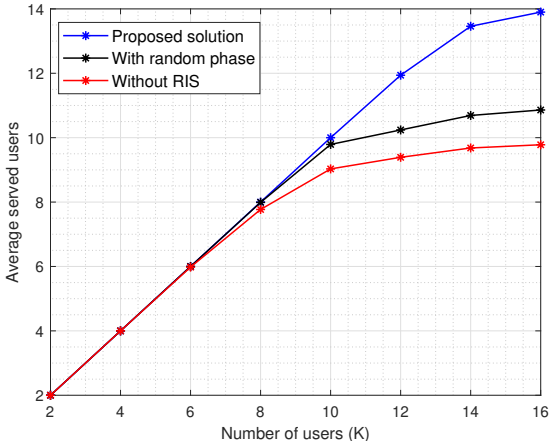

Fig. 5: Average number of served users versus the total number of users, K.

gain is low since the available diversity from the base station direct link is sufficient to serve all users i.e. the RIS cannot provide significant gain. However, when K reaches 16 users, the BS is capable of serving only 10 users on average while it is still possible with optimized RIS for up to 14 users. We obtain a difference of up to 4 more users on average at full loading scenario ($K = M$) compared to the benchmark. In this configuration, even RIS with random phases outperforms the benchmark without RIS by one user on average.

It is evident from the analysis in all the subsections that the joint beamforming leads to substantial performance gains which greatly depends on the channel conditions, e.g. Rician factor, total number of users on the street and position of RIS.

V. Conclusion

We studied the problem of maximizing the number of served users under SINR constraints in a challenging Smart City street scenario. The considered problem involves the joint optimization of the active beamforming at BS and the passive beamforming at the RIS subject to a power constraint at the BS, which is formulated as a mixed-integer non-convex program. Combining tools from alternating optimization and SCA method, we developed an efficient iterative algorithm which guarantees the convergence to at least a local optimal solution. Numerical results have revealed a significant increase in the average number of served users, which is very beneficial for the Smart City application. The gain is especially high with a low Rician factor and large total number of users on the street.

References

[1] Q. Wu and R. Zhang, "Beamforming optimization for wireless network aided by intelligent reflecting surface with discrete phase shifts," *IEEE Trans. Commun.*, vol. 68, no. 3, pp. 1838–1851, 2019.

[2] M. Di Renzo, A. Zappone, M. Debbah, M.-S. Alouini, C. Yuen, J. de Rosny, and S. Tretyakov, "Smart radio environments empowered by reconfigurable intelligent surfaces: How it works, state of research, and the road ahead," *IEEE Sel. Areas. Commun.*, vol. 38, no. 11, pp. 2450–2525, 2020.

[3] Y. Liu, X. Liu, X. Mu, T. Hou, J. Xu, M. Di Renzo, and N. Al-Dhahir, "Reconfigurable intelligent surfaces: Principles and opportunities," *IEEE Commun. Surv. & Tut.*, 2021.

[4] Q. Wu, S. Zhang, B. Zheng, C. You, and R. Zhang, "Intelligent reflecting surface-aided wireless communications: A tutorial," *IEEE Trans. Commun.*, vol. 69, no. 5, pp. 3313–3351, 2021.

[5] N. S. Perović, L.-N. Tran, M. Di Renzo, and M. F. Flanagan, "Achievable rate optimization for mimo systems with reconfigurable intelligent surfaces," *IEEE Trans. Wire. Commun.*, vol. 20, no. 6, pp. 3865–3882, 2021.

[6] X. Qian, M. Di Renzo, J. Liu, A. Kammoun, and M.-S. Alouini, "Beamforming through reconfigurable intelligent surfaces in single-user mimo systems: Snr distribution and scaling laws in the presence of channel fading and phase noise," *IEEE Wire. Commun. Lett.*, vol. 10, no. 1, pp. 77–81, 2020.

[7] Q. Wu and R. Zhang, "Intelligent reflecting surface enhanced wireless network via joint active and passive beamforming," *IEEE Trans. Wire. Commun.*, vol. 18, no. 11, pp. 5394–5409, 2019.

[8] B. N. Silva, M. Khan, and K. Han, "Towards sustainable smart cities: A review of trends, architectures, components, and open challenges in smart cities," *Sustainable Cities and Society*, vol. 38, pp. 697 – 713, 2018.

[9] S. Kisseleff, W. A. Martins, H. Al-Hraishawi, S. Chatzinotas, and B. Ottersten, "Reconfigurable intelligent surfaces for smart cities: Research challenges and opportunities," *IEEE Open J. Commun. Soc.*, vol. 1, pp. 1781–1797, 2020.

[10] E. Basar, M. Di Renzo, J. De Rosny, M. Debbah, M.-S. Alouini, and R. Zhang, "Wireless communications through reconfigurable intelligent surfaces," *IEEE Access*, vol. 7, pp. 116 753–116 773, 2019.

[11] A. Beck, A. Ben-Tal, and L. Tetruashvili, "A sequential parametric convex approximation method with applications to nonconvex truss topology design problems," *J. Global. Optim.*, vol. 47, no. 1, pp. 29–51, May 2010.

[12] A. Bandi, S. Chatzinotas, B. Ottersten *et al.*, "A joint solution for scheduling and precoding in multiuser miso downlink channels," *IEEE Trans. Wire. Commun.*, vol. 19, no. 1, pp. 475–490, 2019.

[13] E. Che, H. D. Tuan, and H. H. Nguyen, "Joint optimization of cooperative beamforming and relay assignment in multi-user wireless relay networks," *IEEE Trans. Wire. Commun.*, vol. 13, no. 10, pp. 5481–5495, 2014.

[14] V.-D. Nguyen, T. Q. Duong, H. D. Tuan, O.-S. Shin, and H. V. Poor, "Spectral and energy efficiencies in full-duplex wireless information and power transfer," *IEEE Trans. Commun.*, vol. 65, no. 5, pp. 2220–2233, May 2017.

[15] A. Ben-Tal and A. Nemirovski, *Lectures on Modern Convex Optimization.* Philadelphia: MPS-SIAM Series on Optimi., SIAM, 2001.

[16] S. W. Ellingson, "Path loss in reconfigurable intelligent surface-enabled channels," in *IEEE Ann. Inter. Symp. Per., Indoor and Mobile Radio Commun. (PIMRC)*, 2021, pp. 829–835.

[17] M. Najafi, V. Jamali, R. Schober, and H. V. Poor, "Physics-based modeling and scalable optimization of large intelligent reflecting surfaces," *IEEE Trans. Commun.*, vol. 69, no. 4, pp. 2673–2691, 2020.

[18] X. Guan, Q. Wu, and R. Zhang, "Intelligent reflecting surface assisted secrecy communication: Is artificial noise helpful or not?" *IEEE Wire. Commun. Lett.*, vol. 9, no. 6, pp. 778–782, 2020.

[19] Ö. Özdogan, E. Björnson, and E. G. Larsson, "Using intelligent reflecting surfaces for rank improvement in mimo communications," in *IEEE Int Conf on Acoustics, Speech and Signal Processing (ICASSP)*. IEEE, 2020, pp. 9160–9164.

[20] C. You, B. Zheng, and R. Zhang, "How to deploy intelligent reflecting surfaces in wireless network: BS-side, user-side, or both sides?" *[Online]: Available at https://arxiv.org/abs/2012.03403*, 2020.